INTERNATIONAL JOURNAL OF SCIENCE AND NATURE

www.scienceandnature.org

DEVELOPMENT OF TRI-METAL OXIDE NANO COMPOSITE ADSORBENTS FOR THE REMOVAL OF REACTIVE YELLOW-15 FROM AQUEOUS SOLUTION

Kamila Banu, N. & *Santhi, T.
Department of Chemistry, Karpagam University, Coimbatore-641021, India,
*Corresponding author email: ssnilasri@yahoo.co.in

ABSTRACT
The use of Zinc, Manganese, Iron mixed metal nano oxide (Zn-Mn-Fe-Nano Oxide metal) as adsorbent to remove Reactive yellow -15 , as a model anionic dye, from aqueous solution was investigated. Zn-Mn-Fe-Nano Oxide metal was prepared by co precipitation and was characterized by XRD, FT-IR and pH zpc . Adsorption experiments were carried out as a function of pH, contact time, concentration of dye, adsorbent dosage, and temperature. The results showed that Zn-Mn-Fe-Nano metal oxide composite was particularly effective to remove Reactive yellow-15 , and that the effective pH range for the dye removal was between 2.0 and 10.0, but at pHs lower than 4pH dissolution of Zn-Mn-Fe-Nano metal oxide composite took place. The adsorption of Reactive yellow-15 on Zn-Mn-Fe-Nano metal oxide composite reached equilibrium within 2 h. The appropriate adsorbent dosage was 1000 mg/L. The interaction between the surface sites of Zn-Mn-Fe-Nano metal oxide composite and the dye ions may be a combination of both anion exchange and surface complexation. Three kinetic models have been evaluated to fit the experimental data. It was shown that the pseudo-second-order model best described the adsorption kinetics of of Reactive yellow-15 onto Zn-Mn-Fe-Nano metal oxide composite. The equilibrium isotherm showed that the adsorption of of Reactive yellow-15 on Zn-Mn-Fe-Nano metal oxide composite of Reactive yellow-15 onto Zn-Mn-Fe-Nano metal oxide composite was consistent with the Langmuir and Freundlich equations. And the saturated adsorption capacity of Reactive yellow-15 onto Zn-Mn-Fe-Nano metal oxide composite for Reactive yellow-15 was 22.73 mg/g.

KEY WORDS: Tri metal oxides nano composite, Reactive yellow-15, equilibrium and kinetic study *etc.*

INTRODUCTION

The effluent discharged from textile dyeing mills consists of highly concentrated dye wastewater with various types of dye. Most dyestuffs are complex aromatic structures, which are difficult to dispose of by natural attenuation. Azo dyes are resistant to biodegradation [1]. Removal of reactive dyes from wastewater is difficult due to their high solubility. These dyes also cause serious ecological problems; for example, they significantly affect the photosynthetic activity of aquatic plants by reducing light penetration, and they may be toxic to some aquatic organisms[2]. There was commonly about 10–15% of unused dyestuff entering the wastewater directly in the dyeing process but the loss of some reactive dyes in the dyeing process can be as high as 50% [3]. Reactive dyes present high solubility and low biodegradability. For these reasons, conventional physiochemical techniques are not capable for reactive dye removal. Therefore adsorption may be employed for the treatment of reactive dye waste [5,6]. Adsorption has significant advantages: low operating cost, high flexibility, simple design and operation, easy automation, lack of sensitivity to toxic pollutants and the capability to operate at very low concentrations [7]. However, it also has some disadvantages: it is a non-destructive technique and it has a high initial cost [8].

Nanotechnology is currently applied in a wide variety of fields, including environmental and wastewater treatment. Nanozerovalent iron (NZVI) technology represents one of the first generations of nanoscale environmental clean-up technologies. Because of its tiny size, its large specific surface area and its high surface reactivity, NZVI can enhance the kinetic rate of destruction of many pollutants [9]. Several applications for environmental clean-up and wastewater treatment by NZVI have been developed, including treatment of TCE (trichloroethylene) and chlorinated ethane[10–12], PCBs (polychlorinated biphenyls) [12,13], 1,2,4-trichlorobenzene [14], p-chlorophenol [15], Acid Black 24 [16] and methyl orange [17].

In this study, a novel Zn-Mn-Fe metal nano oxide composites as adsorbent was synthesized at room temperature, our objective is to develop a facile route to synthesize nanostructured Zn-Mn-Fe metal oxide particles This chemical serves as a morphological control to obtain a high specific surface area and enhance the adsorptive performance of as-synthesized Zn-Mn-Fe nano metal oxides composites . The resulted materials were tested to remove reactive yellow 15 dyes from aqueous solution. The effect of some key factors, such as Zn-Mn-Fe nano metal oxides composite dosage, pH of the solution, contact time and initial concentration of dye on RY-15 removal was also evaluated. A possible mechanism for the formation of Zn-Mn-Fe nano metal oxides composites nanostructured was identifying the XRD and FT-IR results. Adsorptive capacity was assessed by both Langmuir and Freundlich models.

MATERIALS & METHODS

All reagents were of analytical grade and used as received without further purification. Zinc sulphate ($ZnSO_4$) Ferrous sulphate ($FeSO_4$),Manganese di oxide, Sodium hydroxide (NaOH), Reactive yellow-15 (Molecular Formula: $C_{20}H_{20}N_4Na_2O_{11}S_3$ Molecular Weight: 634.57, Λ_{max} = 420nm,denoted as RY-15) were obtained from Sigma-Aldrich. Distilled water was used for preparing all solutions and reagents. All the chemicals used throughout this study were of analytical-grade reagents. All the adsorption experiments were carried out at room temperature (27 ± 2 ^{0}C). The working solutions of different concentrations were prepared by diluting appropriate volume of the original stock solution.

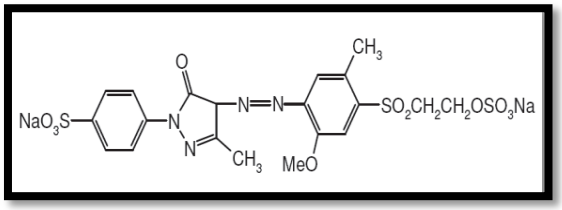

FIGURE1. Structure of Reactive yellow-15

Synthesis and Chaacterization of Zn-Mn-Fe nano oxide composite

In a typical synthesis procedure, metal nano oxides prepared from metal oxides of Zn, Mn, Fe and sulphuric acid were dissolved in distilled water with a molar radio1:1. The solutions were stirred with a Magnetic stirrer at 100^{0}C. Stirring continues till the formation of gel for approximately 2hours.as the gel was formed, it was allowed to burn at 200^{0}C. A light fluffly mass was obtained as a result of combustion.This was further annealed at 1100C for 2 hour to obtain the respective crystalline metal oxide nanoparticles. The metal oxide nanoparticles thus obtained were characterized by x- ray diffraction (XRD), and Fourier-transform infrared (FTIR) spectroscopy. Crystallinity structure and crystallite size of nanoparticles were determined by XRD

Determination of zero point charges (pH_{zpc})

Determination of zero point charge (pH_{zpc}) was done to investigate the surface charge of the adsorbents for various solution pH. About 1 g of the material was prepared in 50 mL solution of sodium nitrate electrolyte of concentration 10^{-2} M. The aliquots of suspension were adjusted to various pH values with dilute NaOH and HNO_3 solution. After 60 minutes for equilibrium, the initial pH value is measured. Then 1 g of $NaNO_3$ was added to each aliquot to bring final electrolyte concentration to about 0.45 M. After an additional 60 minutes agitation, final pH was measured. The results were plotted with pH (final pH - initial pH) against final pH. The pH at which pH is equal to zero is yielded pH zero point charge (pH_{zpc}).

Batch mode studies

The adsorption experiments were carried out as batch tests in an incubator shaker separately for each reactive dye. In a typical batch test, 50 mL dye solution of desired concentration was prepared by suitable dilution of the stock solution and its pH was adjusted using 0.1 M HCl or NaOH solutions. A known amount of dry Zn-Mn-Fe nano oxide composite was then added and the resulting suspension was kept under constant agitation (150rpm) for 2 h in an incubator shaker maintained at a predetermined temperature. After agitation, the solutions were centrifuged at 4000 rpm for 5 min and the absorbance of supernatant solution was recorded using Digital photo calorimeter (model-313). The corresponding concentration in the supernatant solution was obtained using a previously constructed calibration graph. The adsorption capacities were then obtained by using the following mass balance equation.

$$qe = \frac{(Co-Ce)V}{W} \qquad (1)$$

Where C_o and C_e are the initial and equilibrium dye concentrations in solution, V is the solution volume (in L) and W is the weight (in g) of dry adsorbent used.

Analytical technique

The calibration curve for RY-15 obtained by recording absorbance values of dyes solutions in a range of known concentrations at the wavelength of maximum absorbance (λ= 420 nm). Absorbance measurements were taken at a Digital photo calorimeter (model-313)

RESULT & DISCUSSION

Charactrization of Zn-Mn-Fe Nano metal composies:

FTIR measurements are used in order to confirm the formation of Zn-Mn-Fe metal nano- oxide oxide. FTIR spectra, Fig.2 synthesize of Zn-Mn-Fe metal nano- oxide was performed for a better comprehension of the structure and composition of these materials. An absorption band revealing the vibrational properties of Fe bond is observed for in peaks in the range of 3300-3500 cm^{-1} correspond to3400.50-OH group, indicating existence of the hydroxyl groups on the surface of the composites or it can be attributed to the adsorption of some atmospheric water during FTIR measurements. Those at 1625.99 cm^{-1} are the C-O stretching mode of the functional groups on the surface of the Zn-Mn-Fe metal oxide nano- oxide. The two peaks at 2351.23cm^{-1} correspond to the C-H stretch vibration, originated from the surface of composite nano particle.

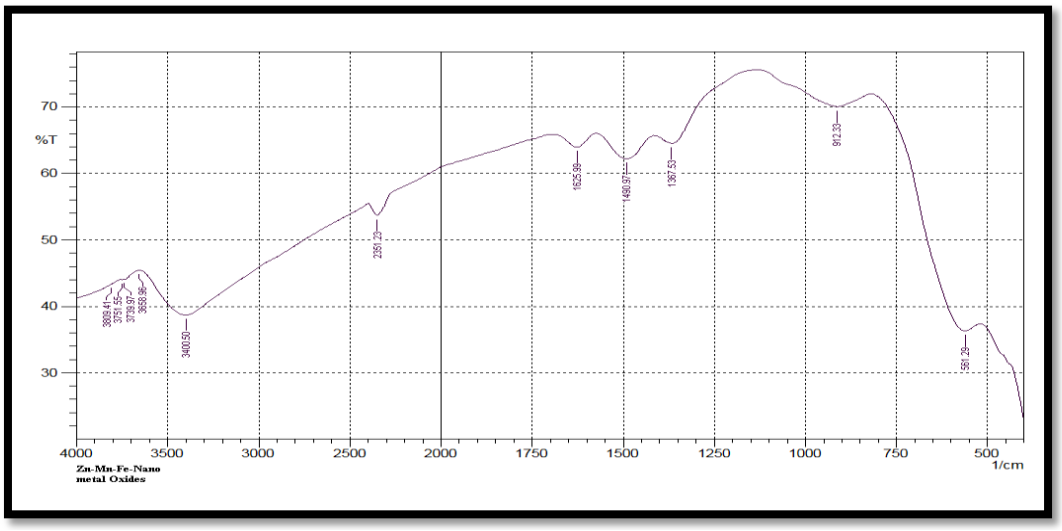

FIGURE 2: FT-IR result of Zn-Mn-Fe-NMOC

Fig.3 shows the XRD images of Zn-Mn-Fe nano oxide composite. The obtained peaks in the position and the relative intensity did not have obvious differences and all of them were for Zn-Mn-Fe nano oxide composite (2Θ = 35.68°). So these results indicate that the modification of Zn-Mn-Fe nano oxide nanoparticles have not changed the crystal structure of nanoparticles, the analysis of powder XRD pattern at room temperature shows that the sample formed is single phase with the hexagonal symmetry. The absence of extra peak claims the purity of the substance and also the complete conversion of Zinc nitrate. The crystalline size of the sample was obtained from Scherer's formula.

$$d = \frac{0.9\lambda}{{}_{\beta}cos\theta} \qquad (2)$$

Where D is the average crystalline diameter, k is a constant (0.9 for Cu-k_),λ--is X-ray wavelength (0.15405 nm for Cu-k_), $_{\beta}$ -is the peak width of half maximum of XRD diffraction lines and Θ- is Bragg's diffraction angle in degree. D values were obtained 32.12nm.respectively.

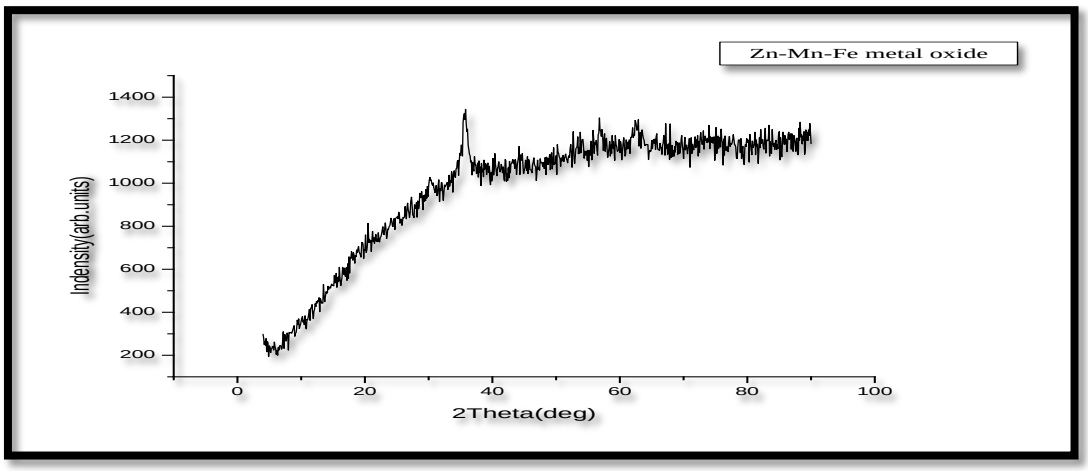

XRD result of Zn-Mn-Fe-NMOC

BATCH STUDY

Effect of pH onto metal oxide composite

An additional batch experiment using 0.2 gL^{-1} Zn-Mn-Fe metal nano oxide composites was conducted to study the effect of pH on decolorization of Reactive Yellow-15 The degradations of dye by different pHs are shown in Fig.4. Resulted in a significant increase in decolorization, more than 56.52%, over the original pH (pH 4). Elevating the pH of Reactive yellow-15 dye aquous solution to 2 to 10 pH resulted. Several factors may explain this trend. The low pH may remove the passivating layers from the RY-15 onto Zn-Mn-Fe metal nano oxide composites [18,19], rendering them free to react with the azo bond in dye molecules. This result may also be ascribed to the pHzpc (zero point charge) of RY-15 onto Zn-Mn-Fe metal nano oxide composites[20] indicated that the pHzpc of Zn-Mn-Fe metal nano oxide composites was around 8.06. At a low pH (<pHzpc), the ZN-Mn-Fe-nano oxide composites surface has positive charge, and the Reactive yellow -15 dye molecules, with a sulfuric group (SO3), have a negative charge[21], attracting the Zn-Mn-Fe metal nano oxide composites particles. Thus, the degradation reaction between the dye molecules and could Zn-Mn-Fe metal nano oxide composites be achieved easily.

On the other hand, at a high pH, Further, at pH>pHPZC the adsorbent became negatively charged and the adsorbate species were positively charged. Under such circumstances, the electrostatic attraction between the

positively charged metal ions and the negatively charged adsorbent surface increases resulting in enhanced adsorption of the adsorbate from the solution. On the other hand, at pH<pHPZC the surface of the adsorbent became positively charged resulting in a decrease in theZn-Mn –Fe-nano metal oxide composite adsorption apparently due to the higher concentration of H^+ ions in the solution that were challenging the positively charged the Zn-Mn –Fe-nano metal oxide composite for the active sites.

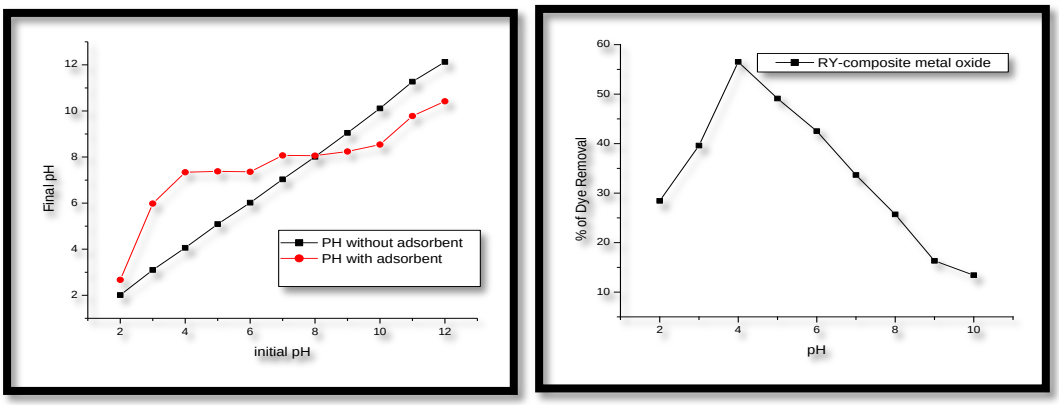

FIGURE 4: Effect of pH of reactive yellow onto Zn-Mn-Fe metal nano oxide composites and zero point of charge-pH_{PZC} of adsorbent(Zn-Mn-Fe-NMOC)

Effect of contact time onto metal oxide composites

The effect of contact time on the adsorption of RY-15 was studied to determine the time taken by Zn-Mn-Fe metal nano oxide composites to remove RY-15 solution at pH 4.0, 0.2 g of Zn-Mn-Fe metal nano oxide composites was added into a 50 mL of RY-15 solution. Absorbance of the solution at 420.00 nm with time was determined to monitor the RY-15 concentration. The decrease in the concentration of RY-15 in the solution with time is due to its adsorption onto Zn-Mn-Fe metal nano oxide composites. Fig. 5 shows that the % RY−15 adsorption increased from 27.11 to 55.93 % as the time increased from 5 min to 110 min. Equilibrium was achieved at 110 min (2 h). The RY-15 adsorption was initially fast upto 75 min, and then it becomes low. The initial rapid adsorption was presumably due to ion exchange with surface hydroxyl ions of the adsorbent. The RY-15 uptake stabilized after a period of 110 min. However, to ensure achievement of equilibrium, for rest of the experiments the contact time was maintained as 2h. . It can be seen that after about 110 min, almost all the RY-15 became adsorbed. Agitation time of 150 min was selected for further works.

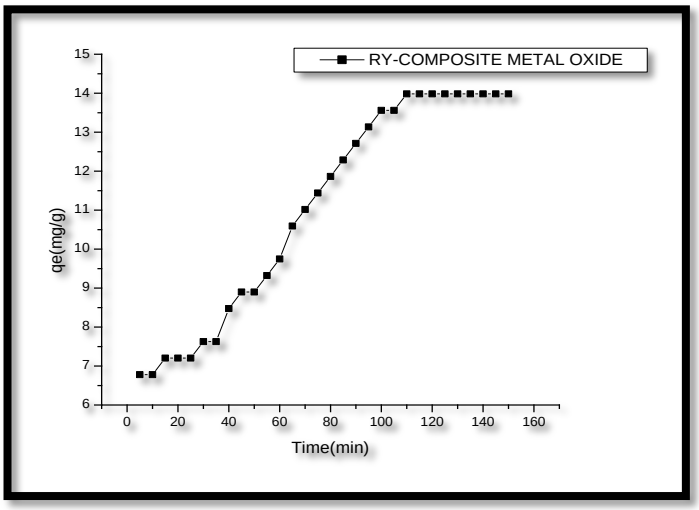

FIGURE 5: Effect of contact time of reactive yellow onto Zn-Mn-Fe metal nano oxide composites

Effect of dose onto metal oxide composite

This study was done for the agents of the Reactive yellow-15 removal with the dosages of 0.5–1.0 g/L at the shown parameters (see Fig. 6). As seen, the removal percent of RY-15 increased with increasing dosage when Zn-Mn-Fe-NMOC was only used. It increased from 56.89% to 74.14% when the dosage of Zn-Mn-Fe-NMOC was increased from 0.20 to 1.0 g/L. It could be due to increasing the reactive sites of Zn-Mn-Fe-NMOC which remove the reactive dye molecules through reduction, generally, viz. an electron transfer process. Therefore, crowding Zn-Mn-Fe-NMOC due to increasing the dosage,

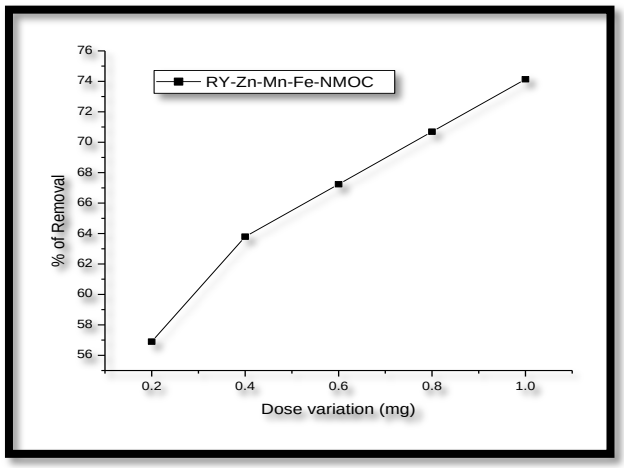

FIGURE 6: Effect of Dose variation of reactive yellow onto Zn-Mn-Fe metal nano oxide composites

Effect of concentration onto metal oxide

The concentration dependence data were shown graphically in Fig. 7 as initial RY-15 concentration against the percent removal of this dye. Increasing the adsorptive concentration apparently caused for a decrease in percent removal of these RY-15 or decreasing the concentration favored for percent uptake of dye removal. This could be ascribed because of the fact that at low adsorptive concentrations, more and more active sites are available for relatively lesser number of adsorbing species. Hence, an enhanced percentage of sorption was observed at low sorptive concentration [21]. More quantitatively, increasing the RY-15 concentration from 25ppm to 200ppm 74 caused for a decrease of percent uptake respectively from 74.57 to 37.28% for RY-15.

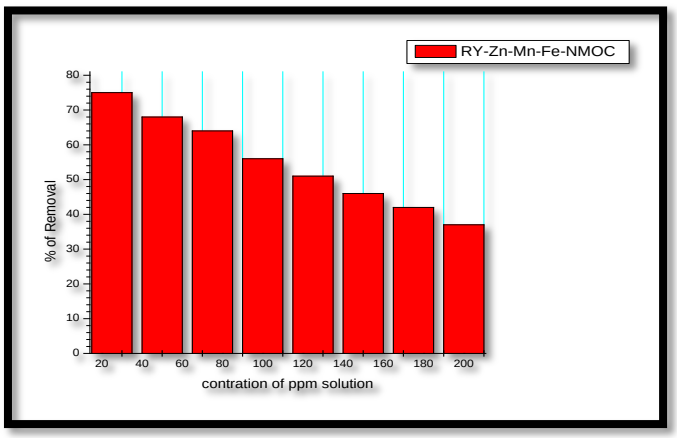

FIGURE 7: Effect of Dye concentration of reactive yellow-15 onto Zn-Mn-Fe metal nano oxide composites

Isotherm models

The equilibrium isotherms describe how the adsorbent interacts with the adsorbate. The correlation of experimental results to adsorption model can help to understand the mechanisms of adsorption and the heterogeneity of the adsorbent surface, and it is also of importance in the practical design and operation of adsorption. Three commonly used isotherm models, namely, Langmuir, Freundlich,Temkin were employed to describe the adsorption of RY-15 . The adsorption isotherm of RY-15 onto Zn-Mn-Fe-NMOC is illustratedin Fig. 8.

Langmuir and Freundlich isotherm models

The batch experimental data were fitted to the Langmuir and Freundlich isotherm models, using a least squares method based on an optimization algorithm. The models are represented mathematically
as follows:

$$C_e/q_e = 1/K_a Q_m + (1/Q_m \times C_e) \quad (3)$$

The Freundlich isotherm model describes the heterogeneous multilayer surfaces of adsorption due to the different trends supporting the surface sites. It supports that occupation will later decrease with the increasing the degree of sites occupation [22]. The well known logarithmic form Freundlich isotherm is given by the following equation.

$$\log q_e = \log K_F + \frac{1}{n}\log C_e \quad (4)$$

where, C_e=equilibrium concentration (mg L^{-1}), q; amount adsorbed per unit weight of carbon(mgg^{-1}).*qe* is the amount of the dye adsorbed by Zn-Mn-Fe-NMOC, *q*m saturated adsorptionof the dye by Zn-Mn-Fe-NMOC ,*K*a constant of the Langmuir isotherm, and *C*e the

concentration of the dye solution. K_f and n are parameters of the Freundlich isotherm Determining the appropriate relationships between equilibrium curves and optimining the design of an adsorption system to remove colored material is essential[23].The equilibrium isotherm (Fig. 8) showed that the adsorption of Ry-15 onto Zn-Mn-Fe-NMOC was consistent with the Langmuir and Freundlich equations, and the correlation coefficient for the Langmuir model was appreciably larger than that for the Freundlich model (R^2 = 0.9981, & R^2 F = 0.9591). The best-fit Langmuir parameters are qm = 22.73 mg/g, K_f = 4.81 L/mg indicates a favorable adsorption process [24]. This result obtained in the Table.2

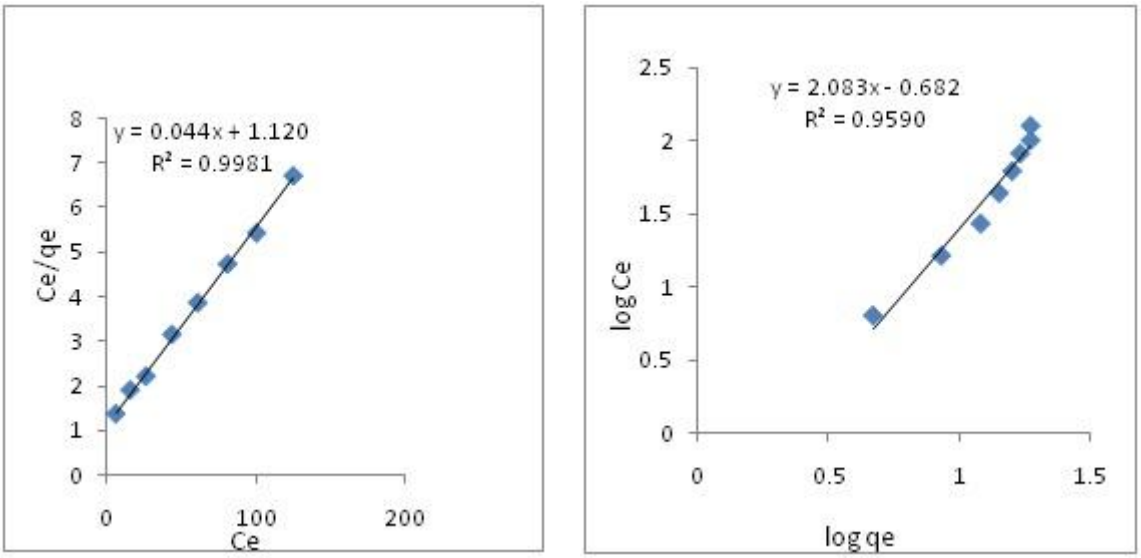

FIGURE 8: Isotherm plots of RY-15 onto Zn-Mn-Fe-NMOC –Langmuir and Freunlich

TABLE 1: Adsorption capacity of dyes on various adsorbent

Dyes	adsorbent	Adsorption capacity(mg/g)	References
Reactive Black 5	Surfactant-modified zeolite	15.9	[25]
Reactive Red 239	Surfactant-modifiedzeolite	12.9	[25]
Acid Blue 29	Fly ash	15.17	[26]
Reactive Blue	Polyurethane foam	8.31	[27]
Vat Blue 4	Smectite-rich clayey rock	17.85	[28]
Reactive Red 141	Zn_2SnO_4	61.0	[29]
Reactive Yellow 145	Chitosan coated magnetic	47.62	[30]
Nanoparticles Biosludge	Vat Black 25	40.0	[31]
	Vat Yellow 1	49.3	[31]
Reactive yellow -15	Zn-Mn-Fe-NMOC	22.73	This work

TABLE 2: Equilibrium model constants for adsorption of RY-15 onto Zn-Mn-Fe-NMOC

Isotherm model			
RY-15+Zn-Mn-Fe-NMOC			
	Langmuir	Freundlich	
Q_m (mgg^{-1})	22.73	1/n	4.81
b (Lmg^{-1})	5×10-2	K_f (mgg^{-1})	2.083
R^2	0.9981	R^2	0.9591

KINETIC STUDY

Pseudo-first-order model

In order to thoroughly understand the adsorption kinetics, two rate equations were applied to evaluate the adsorption of the reactive Yellow-15 dye on Zn-Mn-Fe-NMOC. Pseudo-first-order and pseudo-second-order kinetic models were tested. The adsorption kinetic data were described by the Lagergren pseudo-first-order model [32], which is the earliest known equation describing the adsorption rate based on the adsorption capacity. The differential equation is generally expresses a follows:

$$\frac{dq_t}{d_t} = K_1(q_e - q_t) \quad (5)$$

Where q_e and q_t are the adsorption capacity at equilibrium and at time t, respectively (mg g^{-1}), k_1 is the rate constant of pseudo – first - order adsorption (L min^{-1}). Integrating Eq. (21) for the boundary conditions $t = 0 - t$ and $q_t = 0 - q_t$ gives

$$\log\left(\frac{q_e}{q_e - q_t}\right) = \frac{K_1}{2.303}t \quad 6)$$

Eq. (22) can be rearranged to obtain the following linear form:

$$\log(q_e - q_t) = \log(q_e) - \frac{K_1}{2.303}t \qquad (7)$$

The plot of log(qe −qt) as a function of t provides the k1 and qe values. As shown in Table 3and Fig.9 the correlation coefficients at the 27.5^0 were 0.9180 respectivelCy. However, the linearity is not good and the calculated value of qe is far lower than the experimental qe. This discrepancy shows that the adsorption of RY-15 onto Zn-Mn-Fe-NMOC does not fit the pseudo-first-order kinetic model

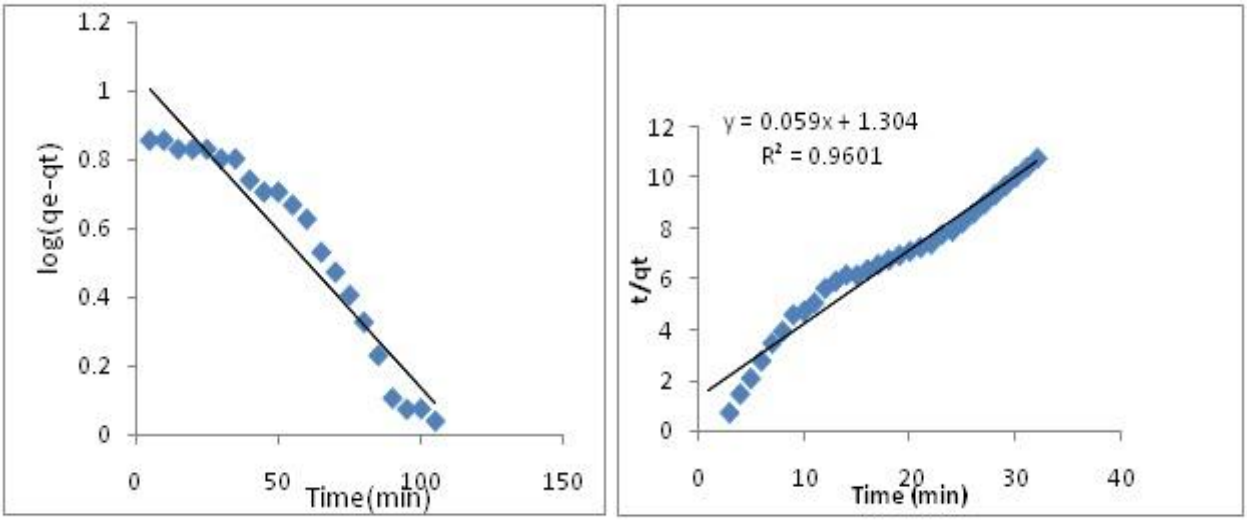

Pseudo-first-order and second order kinetics at different initial concentrations for the adsorption of RY-15 onto Zn-Mn-Fe-NMOS

Pseudo – second - order equation

The adsorption kinetics may be described by the pseudo – second order model [33]. The differential form of the pseudo-second order equation is generally given as follows:

$$\frac{dq_t}{d_t} = K_2(q_e - q_t)^2 \qquad (8)$$

Where k_2 (g (mg min)$^{-1}$) is the second - order rate constant of adsorption. Integrating Eq. (8) for the boundary conditions $q_t = 0 - q_t$ at $t = 0 - t$ is simplified as can be rearranged and linearized to obtain:

$$\frac{t}{q_t} = \frac{1}{K_2 q_e^{\,2}} + \frac{1}{q_e}(t) \qquad (9)$$

The second - order rate constants were used to calculate the initial sorption rate, given by the following equation:

$$h = K_2 q_e^{\,2} \qquad (10)$$

The equilibrium adsorption capacity (q_{eq}), (mg/g) and the second-order constants k_2 (g/mg min), can be determined experimentally from the slope and the intercept of plot *t*/*qt* versus *t*. The applicability of the pseudo-second-order models can be examined by the linear plot of *t*/*qt* versus *t* respectively, as shown in Fig.9. The correlation coefficient R^2 shows that the pseudo-second-order model is indicative of a chemisorptions mechanism, which fits the experimental data slightly better than the pseudo-first-order model. In other words the adsorption of RY-15 (Reactive dye) can be approximated more favorably by the pseudo-second order model. This model has been successfully applied to describe the kinetics of many adsorption systems. The calculated correlations are closer to unity for the second-order kinetics model; therefore, the dye adsorption kinetics could well be more favorably when approximated by a second order kinetic model. The calculated *k*2 (g/mg min) and *q*eq (mg/g) values are listed in Table 4. Kinetic models were tested for RY-15(Reactive dye) onto Zn-Mn-Fe-NMOC (adsorbent) interactions, it was found that the first and second-order kinetic model gave the best fit with the experimental data and therefore, the adsorption followed a mechanism based on order of kinetics. The adsorption coefficients agree well with the conditions supporting favorable adsorption.

The corresponding correlation coefficient (R^2) values for the pseudo – second - order kinetic model were greater than 0.9601 for RY-15 onto Zn-MN-Fe-NMOC, indicating the applicability of the pseudo – second - order kinetic model to describe the adsorption process of RY-15 onto Zn-MN-Fe-NMOC. This led to believe that the pseudo – second - order kinetic model provided good correlation for the adsorption. The higher R^2 values confirm that the sorption process of RY-15 onto Zn-MN-Fe-NMOC follow a pseudo - second - order kinetic model. Similar trends were observed by Sonawane and Shrivastava [34] for dye adsorption onto *Zea mays* (maize) cob, Ahamad and Kumar[35] for adsorption onto ginger waste. It suggested that the adsorption was controlled by chemisorptions.

TABLE 3: Kinetic study of first and second order for adsorption of RY-15 onto Zn-Mn-Fe-NMOC

Adsorbent	C_o (mg/L)	$q_{e\ (exp)}$ (mg/g)	Pseudo-first-order			Pseudo-second-order		
			K_1 min^{-1}	$q_{e(cal)}$ mg/g	R^2	K_2 ($gmg^{-1}min^{-1}$)	$q_{e(cal)}$ mg/g	R^2
Zn-Mn-Fe-MNOC	100	13.98	0.0207	11.21	0.918	0.0824	16.95	0.9601

CONCLUSION

- In this study, the removal of Reactive Yellow-15 dye from aqueous solution using Zn-Mn-Fe-nano metal oxide composite adsorbent was investigated.
- Optimi-zation, parametric studies, adsorption isotherm and kinetic studies were done, and following conclusions were obtained: _ using the Batch mode method, the optimum parameter conditions of 100 ppm initial RY-15 concentration, 2.0 g adsorbent dose and a pH of 4 were determined to yield a maximum RY-15 removal of 56.52%.
- The percent (%) removal of RY-15 was observed to increase with decreasing initial dye concentration and pH, and increasing adsorbent dose. The Langmuir isotherm best described the equilibrium data with R2 = 0.9981, which signifies that a homogeneous adsorp-tion takes place between Reactive yellow-15 and Zn-Mn-Fe-nano metal oxide composite(Zn-Mn-Fe-NMOC) adsorbent
- The pseudo-second order equation best describes the kinetics of the (Zn-Mn-Fe-NMOC) adsorption system due to its high R2 = 0.9601. In addition, the theoretical qe (2.079 mg/g) generated by the pseudo-second order equation is in good agreement with the experimental qe value (13.98 mg/g). This implies that the rate-limiting step is a chemisorption process. This indicates that the rate-determining step is a combination of pore diffusion and chemisorption.
- Conclusively, Zn-Mn-Fe-nano metal oxide composite adsorbent is an effective adsorbent in the removal of RY-15 dye from aqueous solution, where process parameters such as solution pH, initial dye concentration and adsorbent dose significantly affects the 56.52 % of RY-15 removal.

REFERENCES

[1]. Mezohegyi, G., Kolodkin, A., Castro, U. I., Bengoa, C., Stuber, F., Font, J., Fabregat, A., Fortuny, A. (2007) Effective anaerobic decolorazation of azo dye Acid Orange 7 in continuous upflow packed-bed reactor using biological activated carbon system, Industrial Engineering Chemical Research 46: 6788–6792.

[2]. Zollinger (200) Color Chemistry, 3rd ed, Verlag Helvetica Chimica Acta AG, Zurich.

[3]. Easton, J. R., Cooper P. (Ed.) (1995) Colour in dyehouse effluent, Society of Dyers and Colorists, Bradford, 1995, p. 9.

[4]. Al-Degs, Y., Khraisheh, M.A.M., Allen, S.J., Ahmad, M.N., Walker, G.M. (2007) Competitive adsorption of reactive dyes from solution: equilibrium isotherm studies in single and multisolute systems, Chem. Eng. J. 128 (2007) 163–167.

[5]. Ozacar, M., Sengil, I.A. (2003) Adsorption of reactive dyes on calcined alunite from aqueous solutions, J. Hazard. Mater. B98, 211–224.

[6]. Asouhidou, D.D., Triantafyllidis, K.S., Lazaridis, N.K., Matis, K.A., Kim, S.S., Thomas J. Pinnavaia (2009) Sorption of reactive dyes from aqueous solutions by ordered hexagonal and disordered mesoporous carbons, Microporous MesoporousMater. 117: 257–267.

[7]. Gupta, V.K. (2009) Suhas, Application of low-cost adsorbents for dye removal – a review, J. Environ. Manage. 90: 2313–2342.

[8]. Zhang, W. X. (2003) Nanoscale iron particles for environmental remediation: an overview, Journal of Nanoparticle Research 5:323–332.

[9]. H.L. Lien,W.X. Zhang, Nanoscale iron particles for complete reduction of chlorinated ethenes, Colloids and Surfaces A:Physicochemical and Engineering Aspects 191 (2001) 97–105.

[10]. Lio, Y.H., Loa, S.L., Lin, C.J., Kuan, W.H., Weng, S.C. (2005) Chemical reduction of an unbuffered nitrate solution using catalyzed and uncatalyzed nanoscale iron particles, Journal of Hazardous Materials 127 (2005) 102–110.

[11]. Wang, C.B., Zhang, W.X. (1997) Synthesizing nanoscale iron particles for rapid and complete dechlorination of TCE and PCB, Environmental Science & Technology 31: 2154–2156.

[12]. Varanasi, P., Fullana, A., Sidhu, S. (2007) Remediation of PCB contaminated soils using iron nano-particles, Chemosphere 66:1031–1038.

[13]. Zhu, B.W., Lim, T.T., Feng, J. (2006) Reductive dechlorination of 1, 2, 4-trichlorobenzene with palladized nanoscale FeO particles supported on chitosan and silica, Chemosphere 65: 1137–1145.

[14]. Chang, M.C., Shu, H.Y., Yu, H.H. (2006) An integrated technique using zero-valent iron and UV/H2O2 sequential process for complete

decolorization and mineralization of CI Acid Black 24 wastewater, Journal of Hazardous Materials 138: 574–581.

[15]. Shu, H.Y., Chang, M.C., Yu, H.H., Chen, W.H. (2007) Reductive of an azo dye Acid Black 24 solution using synthesized nanoscale zerovalent iron particles, Journal of Colloid and Interface Science 314: 89–97.

[16]. Fan, J., Guo, Y., Wang, J., Fan, M. (2009) Rapid decolorization of azo dye methyl orange in aqueous solution by nanoscale zerovalent iron particles, Journal of Hazardous Materials 166: 904–910.

[17]. Satapanajaru, T., Anurakpongsatorn, P., Pengthamkeerati, P., Boparai, H. (2008) Remediation of atrazine-contaminated soil and water by nano zerovalent iron,Water, Air, and Soil Pollution 192: 349–359.

[18]. Dombek, T., Dolan, F., Schulz, J., Klarup, D. (2001) Rapid reductive dechlorination of atrazine by zero-valent iron under acidic conditions, Environmental Pollution 111: 21–27.

[19]. Li, Z., Jones, H.K., Zhang, P., Bowman, R.S. (2007) Chromate transport though columns packed with surfactant-modified zeolite/zero valent iron pellets, Chemosphere 63:1861–1866.

[20]. Tiwari, D., Mishra, S.P., Mishra, M., Dubey, R.S. (1999) Biosorptive behaviour of Mango (*Mangifera indica*) and Neem (Azadirachta indica) bark for Hg2+, Cr3+ and Cd2+ toxic ions from aqueous solutions: a radiotracer study, Appl. Radiat. Isot. 50: 631–642.

[21]. Aharoni, C., Sparks, D. L. (1991) Kinetics of Soil Chemical Reactions-A Theoretical Treatment. In: D. L. Uarez (Eds.). Rate of Soil Chemical Processes, Soil Science Society of America. Madison.WI.1-18.

[22]. Prasad, A. G. D. and Abdullah, M. A. (2009). Biosorption potential of potato peel waste for the removal of nickel from aqueous solutions: Equilibrium and kinetic studies." International journal of chemical Engineering research. 1(2):77-87.

[23]. Lazaridis, N.K., Asouhidou, D.D. (2003) Kinetics of sorptive removal of chromium (VI) from aqueous solutions by calcined Mg–Al–CO3 hydrotalcite, Water Res. 37: 2875–2882.

[24]. Karadag, D., Turan, M., Akgul, E. (2007) Adsorption equilibrium and kinetics of Reactive Black 5 and Reactive Red 239 in aqueous solution onto surfactant-modified zeolite, J. Chem. Eng. Data 52: 1615–1620.

[25]. Ramakrishna, K. R., Viraraghavan, T. (1997) Dye removal using low cost adsorbents, Water Sci. Technol. 36:189–196.

[26]. Julieta de Jesus da Silveira Neta, Guilherme Costa Moreira, Carlos Juliano da Silva, César Reis, Efraim Lázaro Reis (2011) Use of polyurethane foams for the removal of the Direct Red 80 and Reactive Blue 21 dyes in aqueous medium, Desalination, 281: 55–60.

[27]. Islem Chaari, Mongi Feki, Mounir Medhioub, Jalel bouzid, Emna Fakhfakh, Fakher Jamoussi, Adsorption of a textile dye ''Indanthrene Blue RS (C.I. Vat Blue 4)'' from aqueous solutions onto smectite-rich clayey rock, J. Hazard. Mater. 172 (2009) 1623–1628.

[28]. Edson Luiz Foletto, Gabriela Carvalho Collazzo, Marcio Antonio Mazutti, Sergio Luiz Jahn (2011) Adsorption of textile dye on zinc stannate oxide: equilibrium, kinetic and thermodynamics studies, Sep. Sci. Technol. 46: 2510–2516.

[29]. Nuzhet Ayca Kalkan, Serpil Aksoy, Eda Ayse Aksoy, Nesrin Hasirci (2012) Adsorption of reactive yellow 145 onto chitosan coated magnetite nanoparticles, J. Appl. Polym. Sci. 124: 576–584.

[30]. Allen, S.J., McKay, G., Porter, J.F. (2004) Adsorption isotherm models for basic dye adsorption by peat in single and binary component systems. J Colloid Interface Sci., 280:322.

[31]. Lagergren, S. (1898) on the theory of so called adsorption of dissolved substances. Handlingar, 24, 1 - 39.

[32]. Ho, Y.S, McKay, G., Wase, D.A.J, Foster, C.F. (2000) Study of the sorption of divalent metal ions on to peat, Adsorp. Sci. Technol., 18 639 – 650.

[33]. Sonawane, G. H, Shrivastava, V. S. (2009) Kinetics of decolourization of malachite green from aqueous medium by maize cob (*Zea maize*): An agricultural solid waste. Desalination. 247: 430 – 441.

[34]. Ahmad, R., Kumar, R. (2010) Adsorption studies of hazardous malachite green onto treated ginger waste. J. Environ. Manag., 91: 1032 - 1038.

[35]. Hameed, B.H. (2009a) Spent tea leaves: A non-conventional and low-cost adsorbent for removal of basic dye from aqueous solutions. J. Hazard. Mater. 161: 753 - 759.